Indian Journal of Chemistry
Vol. 54A, December 2015, pp. 1434-1439

Synthesis of ZrO_2 and ZrO_2/SiO_2 particles and photocatalytic degradation of methylene blue

Ali İmran Vaizoğullar[a,] *, Ahmet Balci[b] & Mehmet Uğurlu[b]

[a]Vocat Sch Helth Care, Med Lab Programme, Muğla Sıtkı Koçman University, Muğla, Turkey
Email: vaizogullar@yahoo.com

[b]Department of Chemistry, Faculty of Science, Muğla Sıtkı Koçman University, 48000 Muğla, Turkey

Received 28 May 2015; revised and accepted 24 November 2015

SiO_2 particles (0.6 µm dia.) have been synthesized from tetraethyl orthosilicate and then decorated with ZrO_2 synthesized from zirconium tetrabutoxide. X-ray diffraction, infrared spectra, scanning electron microscopy, energy dispersive X-ray spectroscopy and transmission electron microscopy have been used to characterize the ZrO_2 and ZrO_2/SiO_2 catalysts. The results reveal that there are Si-O-Zr bridges between SiO_2 and ZrO_2 particles and ZrO_2 deposited on the SiO_2 surface. FT-IR analysis shows Si-O-Zr bonding at 1073 cm^{-1}. XRD analysis shows that amorphous SiO_2 and tetragonal ZrO_2 particles are formed at 500 °C. SEM and TEM analyses show that SiO_2 and ZrO_2/SiO_2 nanocomposite particles have a spherical morphology with diameter of 700-750 nm and a uniform particle size. Photoactivity of ZrO_2 and ZrO_2/SiO_2 particles has been investigated in the presence of ozone under UV light with methylene blue as a sample pollutant. Pseudo-first order kinetic model gives R^2 values to be 0.69-0.97 and 0.79-0.93 for ZrO_2 and ZrO_2/SiO_2 respectively. This study proves that ozone assisted ZrO_2/SiO_2 catalyst is an effective and fast-reacting system for photocatalytic removal of organic pollutants present in wastewater.

Keywords: Photocatalytic degradation, Dye degradation, Composites, Nanocomposites, Zirconia, Silica, Methylene blue

Composite particles are being effectively used as chemical components in many applications such as catalyst, electromagnetic fields, photocatalytic degradation etc[1-5]. The composites with properties have been the focus of extensive research.[6,7] There are many methods such as thermal evaporation, electroless plating, sol–gel method and via encapsulation[8,9] to synthesize composite particles. However, the most common methods are sol-gel and vacuum evaporation[10].

Industrial wastes such as rubber, paper, plastics and food cause environmental pollution due to azo dyes[11]. These azo dyes significantly affect the water quality[12] and cause diseases such as cancer which affects the health of people and other living things[13]. Recently, photocatalytic degradation method was used as an effective method for the elimination of azo dyes[14]. In this, semiconductor composite materials play an important role in the photocatalytic process.

ZrO_2 is an n-type semiconductor oxide and its photocatalytic activity has been successfully tested by Herrman *et al.*[15] Relatively wide band gap value and the high negative value of the conduction band allow it to be used as a photocatalyst in the production of hydrogen through water decomposition[16]. In ZrO_2/SiO_2 related studies, researchers have focused on the design of composite particles and even the deposition of ZrO_2 on spherical SiO_2 surfaces. However, there are no photocatalytic studies with ZrO_2/SiO_2 mixed oxide. In addition, ozone assisted ZrO_2/SiO_2 catalyst has not been studied for photocatalytic application under UV light.

In the present study, we have synthesized ZrO_2 and ZrO_2/SiO_2 spherical nanocomposite catalysts by using a simple sol–gel process. The structure and texture are characterized by FT-IR, SEM-EDAX, TEM and XRD techniques, and their photocatalytic activity has been assessed using methylene blue (MB) as a sample pollutant. The suspension *p*H, catalyst concentration and temperature were kept constant in all experiments. We have also investigated how SiO_2 and ozone affect the photocatalytic activity of ZrO_2 in the spherical composite form.

Materials and Methods

Preparation of SiO_2 and ZrO_2 particles and ZrO_2/SiO_2 nanocomposite

SiO_2 particles were synthesized by using sol-gel method. Initially, 50 mL NH_3 solution and 25 mL absolute ethanol and 50 mL water were mixed.

Then, 20 mL tetraethyl orthosilicate was added to this solution drop by drop and mixed for 4 h. The particles obtained were filtered and washed with water three times and dried at 80 °C in an oven and calcined for 3 h.

For ZrO_2 particles, 10 mL zirconium tetrabutoxide was dissolved in 150 mL aqueous ethanol and then ammonia solution was added drop by drop to this mixture. The *p*H was adjusted to 6 and then mixed for 12 h. The obtained solution was filtered and calcined at 500 °C for 3 h.

For synthesizing ZrO_2/SiO_2 spherical nanocomposite particles, SiO_2 particles (1 g) obtained by the above procedure were added to ethanol-water mixture (50 mL), then 20 mL TBOZ and 30 mL ethanol were added to the solution and mixed for 3 h. The obtained particles were filtered and calcined at 500 °C, washed three times and dried in an oven at 80 °C for 12 h.

Characterization

The crystalline phase structure of the sample was examined by XRD (Rigaku-Smart Lab) using copper K radiation (λ = 0.154056 nm). The FT-IR spectra these particles were recorded on Thermo-Scientific, (Nicolet IS10-ATR) spectrophotometers. The size and shape of the particles were investigated by SEM (JEOL JSM-7600F) and TEM (JEOL JEM 2100F HRTEM). Elemental analysis was carried out using (JEOL JSM-7600F) EDAX analyzer with SEM. The Brunauer-Emmett-Teller (BET) surface area was measured using ASAP 2010 (Micromeritics Instrument Corporation, USA) with N_2 adsorption at 77.35 K.

Particle size was determined from X-ray diffraction analysis, carried out using Cu-Kα radiation (1.540 Å). The crystallite size of ZrO_2 and ZrO_2/SiO_2 spherical nanocomposite particles were calculated Å using Scherer equation; $d = B \,/\, _{1/2}\cos$ where d is the average particle size, B is the Scherrer constant (0.91), λ is wavelength of the radiation $\beta_{1/2}$ is full width at half maximum of the diffraction peak and θ is the diffraction is the diffraction angle.

The band gap energies of samples were determined by the diffuse reflectance spectra recorded on UV-visible-DRS Shimadzu spectrophotometer in the wavelength range of 200-800 nm. The approximate optical band gap (Eg) was determined as $Eg = 1240/\lambda$.

Photocatalytic studies

The aqueous solution of MB was prepared by dissolving known quantity of $C_{16}H_{18}ClN_3S.xH_2O$ (Fluka, 97%) in doubly distilled water. It was further diluted to obtain standard solutions. All the reagents used were of analytical grade.

In photolytic experiments, a specially designed UV reactor was used. This reactor consists of a closed system having an UV lamp, properties of fixed mixing and water cooling and ozone entry (Fig. 1). The color of MB was analyzed by using Dr. Lange spectrophotometer and maximum wavelength in the visible area was determined to be 664 nm. All color changes were investigated at this wavelength. All photocatalytic experiments were carried out in UV reactor under the following experimental conditions. The amount of catalyst, ozone flow rate, and concentration of MB and volume of MB solution were: 1 g, 1.5 g/mL, 50 mg/L and 50 mL respectively.

The amount of degradation was calculated every 30 min. The degradation percentage of MB was calculated as: %Degradation = $\{(C_0 - C)/C_0\}$, where C_o is the initial concentration of MB and C is the MB concentration at time t. Degradation efficiency was compared from the difference between degradation percentages of each parameter.

Results and Discussion

XRD analysis of ZrO_2 and ZrO_2/SiO_2 particles

Figure 2 shows XRD pattern of the ZrO_2, SiO_2 and ZrO_2/SiO_2 spherical nanocomposite particles respectively. In Fig. 2a the XRD patterns of ZrO_2 show peaks appearing at 2θ: 28.09°, 30.08°,

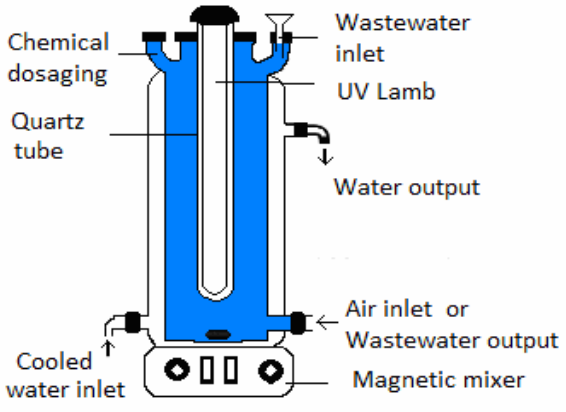

Fig. 1 – Schematic representation of UV reactor used in the present study.

31.23°, 35.19°, attribute to the tetragonal ZrO_2 (JCPDS-17-0923). There is only one broad peak centered at 2θ = 23.42°, suggesting that amorphous SiO_2 was formed during calcination at 500 °C (Fig. 2b). For ZrO_2/SiO_2 spherical nanocomposite particles, there are four peaks appearing at 2θ: 28.09°, 30.13°, 31.26°, 34.42°, corresponding to the tetragonal ZrO_2[17] besides one peak at 23.81°, which may be attributed to amorphous SiO_2 (Fig. 2c). This indicates that the transformation of ZrO_2 from *t*-ZrO_2 to *m*-ZrO_2 does not occur because of stabilization of tetragonal ZrO_2 by SiO_2. Calculated

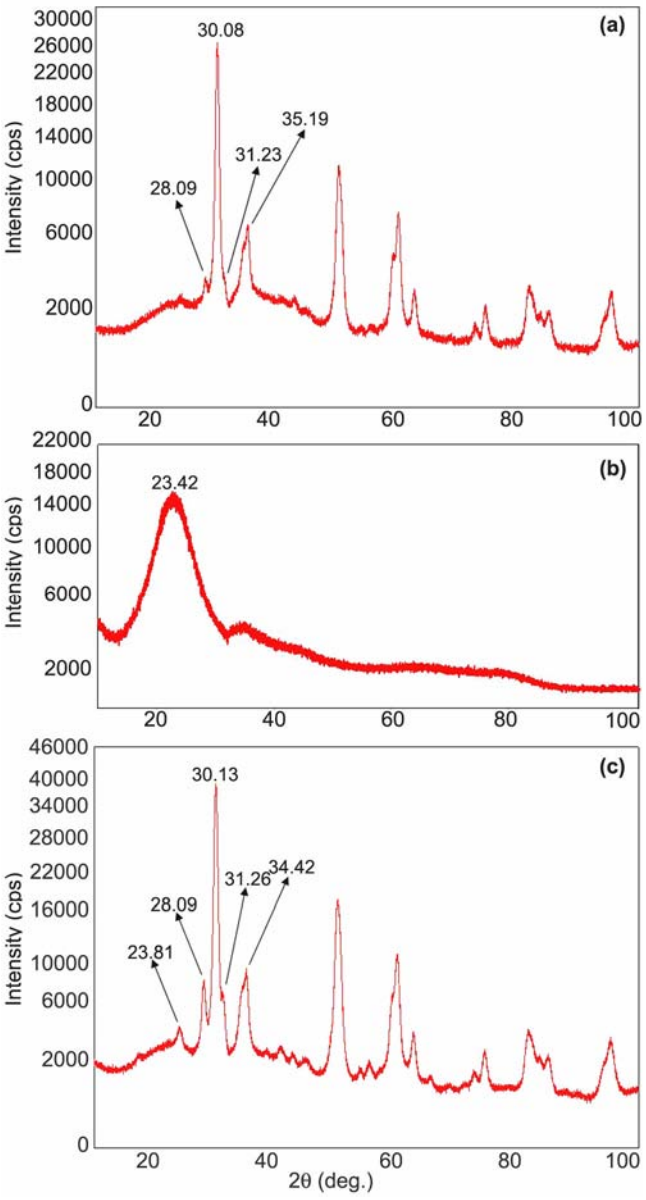

Fig. 2 – XRD patterns of (a) ZrO_2 particles, (b) SiO_2 particles, and, (c) ZrO_2/SiO_2 particles.

crystalline size from XRD analysis showed particle size to be 1.12 nm for SiO_2 particles and 11.52 nm for ZrO_2/SiO_2 spherical nanocomposite particles.

FT-IR analysis

The presence of chemical bonding between SiO_2 and ZrO_2 was investigated with FT-IR analysis. Si-O-Si asymmetric stretching at 1100 cm^{-1} corresponding to SiO_2 is observed. The characteristic peaks of Si–OH at 799 cm^{-1} may be attributed to the silanol groups on the SiO_2 particles. In both spectra, the peaks which appear at about 3226 cm^{-1} and 3381cm^{-1} are due to the bending vibration of OH from water. In the FT-IR spectrum of ZrO_2/SiO_2 spherical nanocomposite particles, it was observed that the peak shifted from 1100 cm^{-1} to 1073 cm^{-1}. According to Zhan *et al.*[18] and Lee *et al.*[19] this shift arises from zirconia in a Si-O-Zr bond because of strong electropositivity of ZrO_2. Dang *et al.*[20] reported that stretching vibration modes of Zr-O-Si bonds may be assigned at 967 cm^{-1}; however an increase in the number of Si-O-Zr bonds leads to increased shifts in FT-IR spectrum. Chen *et al.*[21] reported that Si-O-Zr bonds can be assigned at 1050 cm^{-1} which is attributed to the silica network forming the Si-O-Zr band. These reports are consistent with our findings and verified the oxygen bridge between Si and Zr.

SEM and EDAX

SEM images of SiO_2 and ZrO_2/SiO_2 nanocomposite microsphere were recorded (Fig. 3). Smooth and co-shaped SiO_2 particles are observed. The average diameter of ZrO_2/SiO_2 spherical nanocomposite particles is increased due to the ZrO_2 on the SiO_2 surface (Fig. 3(b,c)). EDAX analysis shows the qualitative presence of Zr, O, and Si as the main elements and confirms that ZrO_2 particles are on the surface of SiO_2 particles (Fig. 4).

TEM analysis

Figure 5 shows the TEM image of ZrO_2/SiO_2 spherical nanocomposite particles. The presence of ZrO_2 on SiO_2 surface with roughness was clearly observed. Self-aggregations of ZrO_2 occurred because of high generation rate of ZrO_2 particles. Therefore, the rate of generation of ZrO_2 particles during the hydrolysis and condensation reactions must be controlled in the sol-gel process[21].

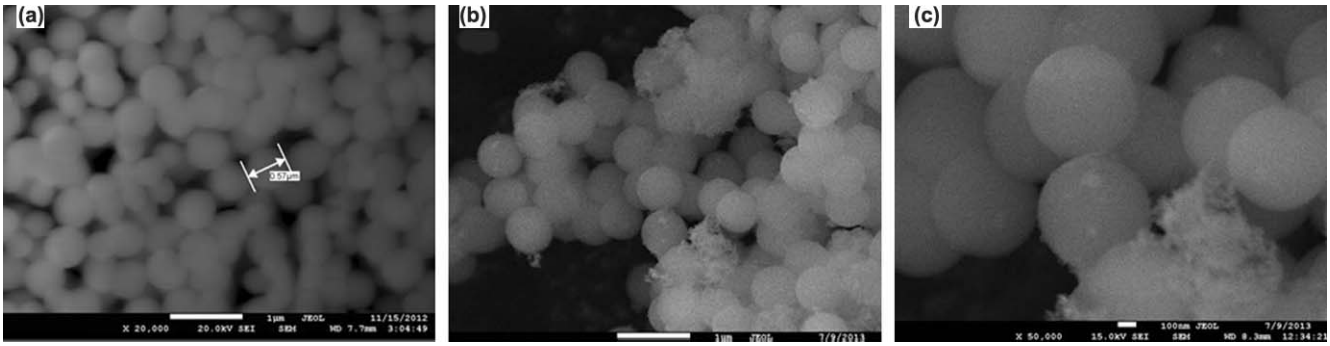

Fig. 3 – SEM images of (a) SiO_2 particles, and, (b,c) ZrO_2/SiO_2 particles.

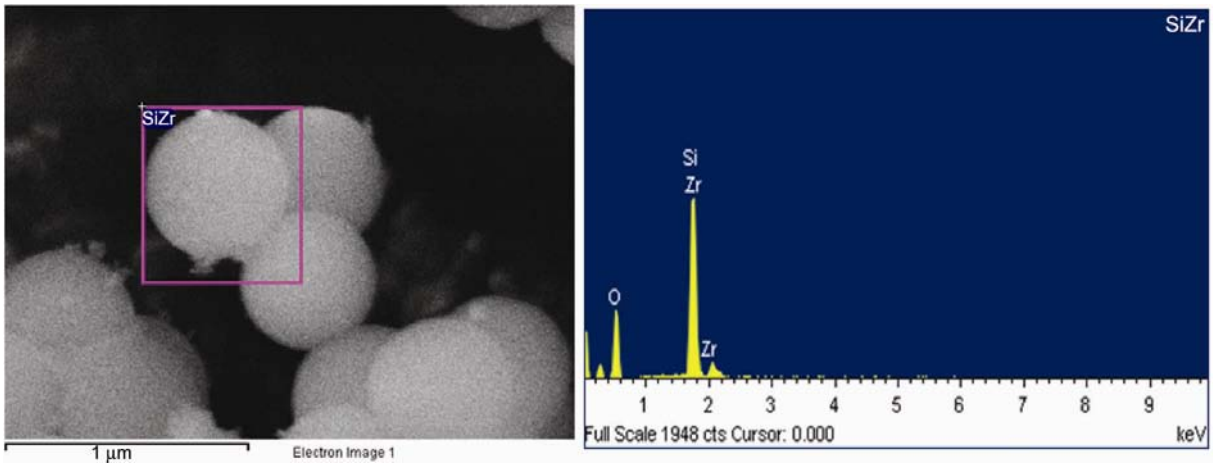

Fig. 4 – EDAX analysis of ZrO_2/SiO_2 particles.

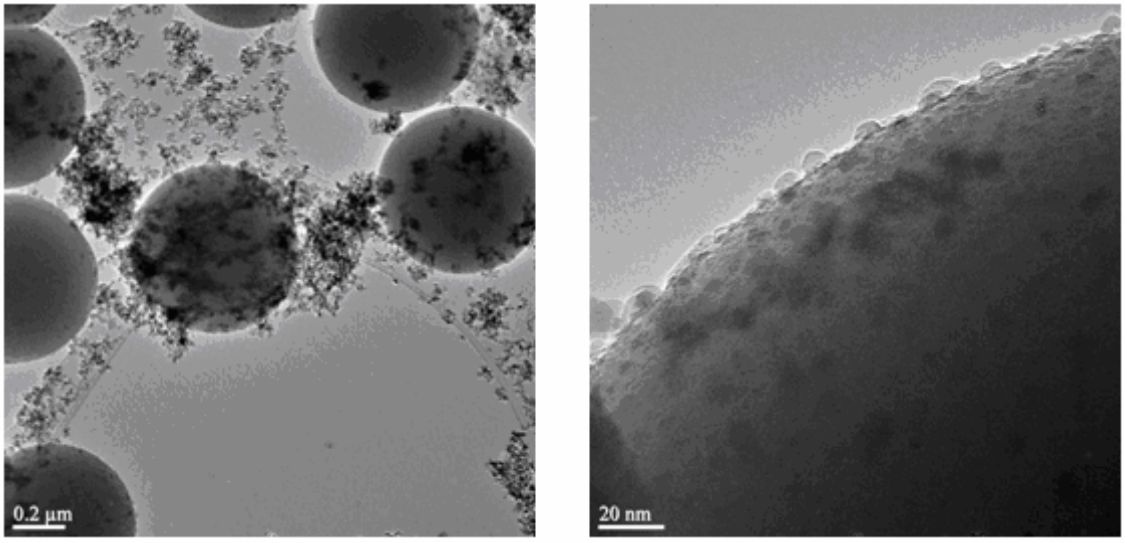

Fig. 5 – TEM analysis of ZrO_2/SiO_2 particles.

Table 1 – Kinetic parameters for the degradation of MB by ZrO_2 and ZrO_2/SiO_2 particles as catalyst

System	ZrO_2		ZrO_2 /SiO_2	
	R^2	$k\times10^{-3}(min^{-1})$	R^2	$k\times10^{-3}(min^{-1})$
UV	0.69	0.20	0.79	0.21
Catalyst only	0.69	0.21	0.78	0.23
UV/Catalyst	0.82	3.54	0.96	5.81
UV/O_3	0.94	4.71	0.95	7.91
UV/O_3/Catalyst	0.97	11.01	0.93	31.90

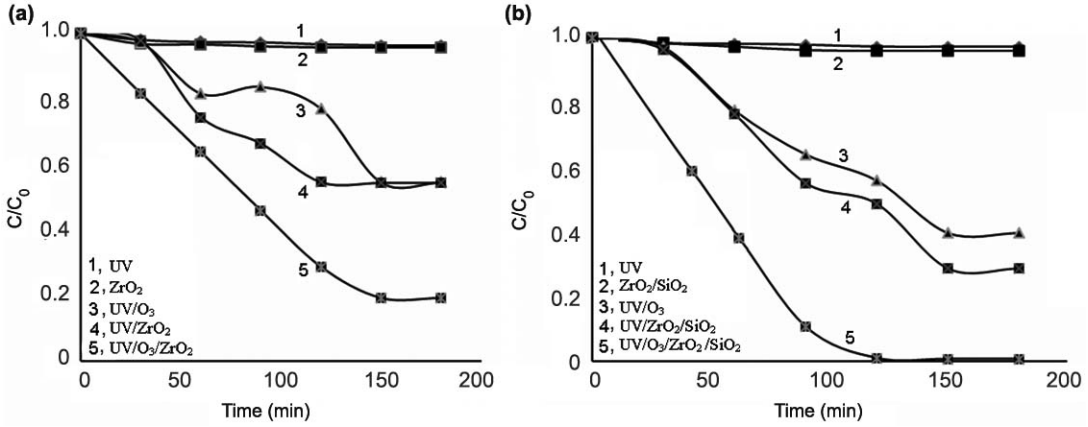

Fig. 6 – Photocatalytic degradation rates of MB with (a) ZrO_2 particles, and, (b) ZrO_2/SiO_2 particles.

Photocatalytic activity

The photoactivity of ZrO_2 and ZrO_2/SiO_2 nanocomposite microsphere particles for degradation of MB was investigated and the obtained results are shown in Fig. 6. The experiments were carried out at naturel *p*H = 7, 10 mg/L catalyst and at 298 K. Illumination solutions were mixed in dark by with magnetic stirring for an hour. The photodegradation was studied by monitoring the absorbance of the MB solution at the maximum absorption wavelength of 664 nm. After the photocatalytic studies, the amount of degradation was calculated with C/C_o, where C_o was initial concentration of MB and C was the concentration in solution at time.

The pseudo-first order kinetic model explains the kinetics of photocatalytic degradation of MB $\ln(C_0/C) = kt$. The first order kinetic constant k (1/min) for MB degradation was calculated by plotting $\ln(C_0/C)$ versus time (t). From Table 1, it can be clearly observed that pseudo-first order kinetic constant increased and reached to 11.1 and 31.9 for UV/O_3/ZrO_2 and UV/O_3/ZrO_2/SiO_2 catalyst respectively. UV/O_3/ZrO_2/SiO_2 catalyst with $k = 31.9\text{x}10^{-3}$ (which is about three times that of UV/O_3/ZrO_2) shows the highest MB degradation rate.

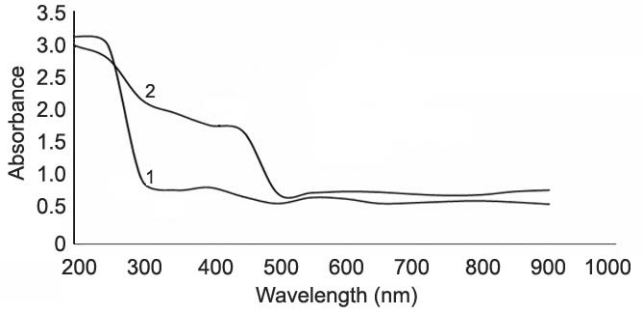

Fig. 7 – UV-visible DRS reflectance spectra of ZrO_2 (curve 1) and SiO_2/ZrO_2 (curve 2).

The band gap values of ZrO_2 and SiO_2/ZrO_2 catalyst were calculated to be 4.13 eV and 2.48 eV respectively (Fig. 7). The band absorptions of the SiO_2/ZrO_2 spherical nanocomposite particles shift to longer wavelengths, indicating decrease in the band gap level. In this case, more photogenerated e^-/h^+ pairs are involved in the photocatalytic reactions.

ZrO_2 exhibit low photoactivity because of low absorbance in the UV range [22]. When photo-activity of ZrO_2 is compared with that of ZrO_2/SiO_2 particles, it is seen that ZrO_2/SiO_2 spherical nanocomposite particles were more active than ZrO_2 because of lattice deformation which is confirmed by unchanged t-ZrO_2 phases from the XRD results[23] during the

formation of Si-O-Zr and Si-O^- bonds. The lattice deformation caused the band gap energy of ZrO_2 (*Eg*) to shift to lower energy due to strain at SiO_2/ZrO_2 interface which provides an easier excitation of the electrons of ZrO_2 resulting in more effective photoactivity.

In addition, SiO_2 provides the better dispersion stability which allows increased contact of MB molecules with the catalyst surface per unit time. Both particles did not show any photoactivity under only UV and only catalyst conditions however we observed that O_3 (ozone) degraded some MB even without catalyst. This can be explained as ozone transforming into O_2 and OH^- being used to oxidize organic molecules and chlorinated organic compounds[24].

$$O_3 + H_2O + 2e^- \longrightarrow O_2 + 2OH^-$$

The BET surface area of SiO_2, ZrO_2, and ZrO_2/SiO_2 are 159.4, 23.5 and 52.3 m^2/g respectively. Compared to that of SiO_2, the surface area of ZrO_2/SiO_2 decreases due to agglomeration of ZrO_2 particles on the SiO_2 surface, which can be clearly seen from SEM images.

We noticed that the best photoactivity under the experimental conditions occurred on using $UV/O_3/ZrO_2/SiO_2$ catalyst. In general, the photocatalytic reaction begins when photons excited electrons from valence band to conductivity band in semiconductor materials, then continues with the diffusion of charge carriers to the particle surface where the reaction with water molecules reveals highly reactive species of peroxide (O_2^-) and hydroxyl radical (OH^*) responsible for the degradation of adsorbed organic molecules[25].

Ozone used in the photocatalytic degradation produce O_2 molecule and OH^- ion which cause formation of peroxide and hydroxyl radicals in conductivity and valence band respectively; in this case photocatalytic efficiency increases because of peroxide and hydroxyl radicals from both ozone and adsorbed water.

The photocatalytic reactions for degradation of MB can be expressed as:

$$ZrO_2{}^* + h\nu \longrightarrow ZrO_2\ (h^+ + e^-)$$

$$h^+ + OH^- \longrightarrow OH^*\ (OH^* \text{from both } O_3 \text{ and water})$$

$$e^- + O_{2ads} \longrightarrow O_2{}^-_{ads}\ (O_2^- \text{from both } O_3 \text{ and water})$$

Conclusions

SiO_2 particles decorated with ZrO_2 particles were obtained using sol-gel method. Electron microscopy X-ray diffraction and infrared spectroscopy were used to reveal the presence of Si-O-Zr bridges between SiO_2 and ZrO_2 particles. The particle size of ZrO_2 on SiO_2 surface was ~10 nm. Compared with ZrO_2, the ZrO_2/SiO_2 spherical nanocomposite microspheres exhibit enhanced photocatalytic efficiency. Ozone contributed to the photoactivity of catalyst by producing peroxide and hydroxyl radicals.

References

1 Guo X C & Dong P, *Langmuir,* 15 (1999) 5535.
2 Guo X C, Zhao P, Guo H L & Zhao Q, *Langmuir,* 19 (2003) 9799.
3 Guo H X & Zhao X P, *Opt Mater,* 22 (2003) 39.
4 Guo H X, Zhao X P, Ning G H & Liu G Q, *Langmuir,* 19 (2003) 4884.
5 Xia Y, Gates B & Li ZY, *Adv Mater,* 13 (2001) 409.
6 Matijevic E, *Langmuir,* 10 (1994) 8.
7 Caruso F, *Adv Mater,* 13 (2001) 11.
8 Liu G Y, Yang X L & WangY M, *Polymer,* 48 (2007) 4385.
9 Yu D G, An J H, Bae J Y, Kim S, Lee Y E, Ahn S D, Kang S Y & Suh K S, *Colloid Surf: A,* 245 (2004) 29.
10 Rubio F, Rubio J & Oteo J L, *J Mater Sci Lett,* 16 (1997) 49.
11 Somiya S, Yamamoto N &Yanagina H, *Adv Ceram,* 24 (1988) .
12 Rahulan K M, Vinithab G, Devaraj S L & Kanakam C C, *Ceram Int,* 39 (2013) 5281.
13 Nawale A B, Kanhe N S, Bhoraskar S V, Mathe V L & Das A K, *Mater Res Bull,* 47 (2012) 3432.
14 Sun J H, Wang Y K, Sun R X & Dong S Y, *Mater Chem Phys,* 115 (2009) 303.
15 Herrman J M, Disdier J & Pichat P, *J Chem Soc Faraday Trans,* 77 (1981) 2815.
16 Kumar S, Animesh K & Ojha A K, *J Alloys Compd,* 644 (2015) 654.
17 Qu X, Xie D, Lao C & Dua F, *Ceram Int,* 40 (2014) 2647.
18 Zhan Z & Zeng H G, *J Non-Cryst Solids,* 243 (1999) 26.
19 Lee S W & Condrate R A, *J Mater Sci,* 23 (1988) 2951.
20 Dang Z, Anderson B G, Amenomiya Y & Morrow B A, *J Phys Chem A,* 99 (1995) 14437.
21 Chen R & Song X, *J Chinese Chem Soc,* 51 (2004) 945.
22 Xie S B, İglesia E & Bell A T, *Chem Mater,* 12 (8) (2000) 2442.
23 Vasanthavel S, Kumar P N & Kannan S, *J Am Ceram Soc,* 97 (2014) 635.
24 *EPA Guidance Manual, Alter Disinfec and Oxidants,* April 1999.
25 Kadi M W & Mohamed R M, *Int J Photoenergy,* 812097 (2013) 7.